the plane of the boundary are considered. In particular the effect of **t** on the structure of a grain boundary is ignored, or at least not explicitly considered. For instance, for a bicrystal to be in a c.s.l. orientation it is necessary that $\mathbf{t}=0$. This is implied by the existence of common lattice points (*cf.* §2). Even when the axis/angle pair has the correct values for the existence of a c.s.l., it is necessary that $\mathbf{t}=0$ for a c.s.l. boundary to occur. Fig. 1 shows how the parameter **t** can profoundly change the atomic configuration at the boundary.

The necessity of so many parameters to characterize a grain boundary, together with the fact that small fluctuations of the boundary parameters may drastically affect the properties of grain boundaries, make the experimental determination of the parameters a difficult and important question. The methods generally employed (diffraction techniques) do not provide complete information on the relative orientation of the two crystals and on the location of the boundary. They only give the direction of the axis of misorientation and the value of θ, while **t** remains undetermined. Field-ion microscopy is probably unique in providing complete information on the grain boundary parameters (*cf.* Fortes & Smith, 1970).

References

BISHOP, G. H. & CHALMERS, B. (1968). *Scripta Met.* **3**, 133.
BRANDON, D. G. (1966). *Acta Met.* **14**, 1479.
BRANDON, D. G., RALPH, B., RANGANATHAN, S. & WALD, M. (1964). *Acta Met.* **12**, 813.
FORTES, M. A. & SMITH, D. A. (1970). *J. Appl. Phys.* **41**, 2348.
GOUX, C. (1961). *Mem. Sci. Rev. Mét.* **58**, 661.
RANGANATHAN, S. (1966). *Acta Cryst.* **21**, 197.

Acta Cryst. (1972). A**28**, 102

The Theory of X-ray Crystal Diffraction for Finite Polyhedral Crystals. I. The Laue–Bragg Cases

BY T. SAKA, T. KATAGAWA AND N. KATO

Department of Applied Physics, Faculty of Engineering, Nagoya University, Nagoya, Japan

(*Received* 18 *January* 1971 *and in revised form* 7 *July* 1971)

The entrance and exit surfaces are defined with respect to the Poynting vector, and the Bragg and Laue cases are redefined separately with respect to the wave vector on the entrance and exit surfaces. In this paper, the diffraction phenomena in the Laue (on the entrance surface)–Bragg (on the exit surface) case are discussed on the basis of both the plane-wave and spherical-wave theories. The two-beam approximation is used throughout, by taking account of absorption. Total reflexion is expected on the exit surface inside the crystal for either direct or Bragg-reflected waves. The wave fields in the spherical-wave theory are represented by Bessel functions, in the forms which are very similar to the Laue case (Kato, *J. Appl. Phys.* (1968). **39**, 2225). This implies that the reflected waves are regarded as a divergent cylindrical wave starting from an imaginary focal point. The treatments described here are easily extended to more general cases in plane-bounded crystals. In this sense, this paper is a preparation for treating the diffraction phenomena in a finite polyhedral crystal.

Introduction

The phenomena of Pendellösung in crystal diffraction were originally predicted by Ewald (1916) and observed first by Kato & Lang (1959) in the X-ray case. Kato (1961*a*,*b*) has interpreted theoretically the observed fringe pattern by regarding the incident wave as a spherical wave. This theory is called 'spherical-wave theory' and the corrcsponding wave fields are called 'spherical-wave solutions'. The conventional theory in which the incident wave is regarded as a plane wave is called 'plane-wave theory' and the corresponding wave fields called 'plane-wave solutions'. Later, Kato, Usami & Katagawa (1967) extended the spherical-wave theory to the case of the crystal including a stacking fault.

In the above theories, although the exit surface is not necessarily parallel to the entrance surface, it is assumed that both *O* (direct) and *G* (Bragg-reflected) waves pass through the exit surface. In general cases, however, one of the *O* and *G* waves cannot pass through the exit surface when it is nearly parallel to the lattice plane concerned. In fact, Borrmann, Hildebrandt & Wagner (1955), Borrmann & Lehmann (1963) and Lehmann & Borrmann (1967) have studied experimentally diffraction phenomena under this condition. They have also considered the plane-wave theory for a special geometry* and highly absorbing crystals.

* A symmetrical Laue case in which the lattice plane is perpendicular to the entrance surface and parallel to the exit surface.

Here, we shall treat this problem in the general case from the viewpoints of both plane-wave and spherical-wave theories. The method used is similar to that used in the previous theories of Kato, Usami & Katagawa (1967). First, the plane-wave solution is obtained and, next, the spherical-wave solution is represented as a superposition of the plane-wave solution. In the present case, contrary to the case of stacking faults, the integrals required are obtained rigorously in terms of Bessel functions.

The present series of papers is intended to develop the spherical-wave theory already worked out in the Laue case, in order to describe the diffraction phenomena in a finite crystal bounded by plane surfaces. This paper, however, is only concerned with the simplest but most fundamental case in which the crystal is bounded by one entrance and one exit surface. This theory assumes that the incident wave creates one G wave under the Laue case condition on the entrance surface and that the crystal wave arrives at the exit surface under the Bragg case condition. The more general cases and the case in which the incident wave falls on an entrance surface under the Bragg case condition will be treated in succeeding papers. It should be pointed out that the same problem is considered by Uragami (Bragg case: 1969, 1970; Laue: 1971) on the basis of Takagi's (1969) approach to crystal diffraction.

New definitions of the Laue and Bragg cases

Before going into details, it seems desirable to clarify the concepts of 'the entrance and exit surfaces' and to re-define 'the Laue and Bragg cases' in a way suitable for further development of the theory.

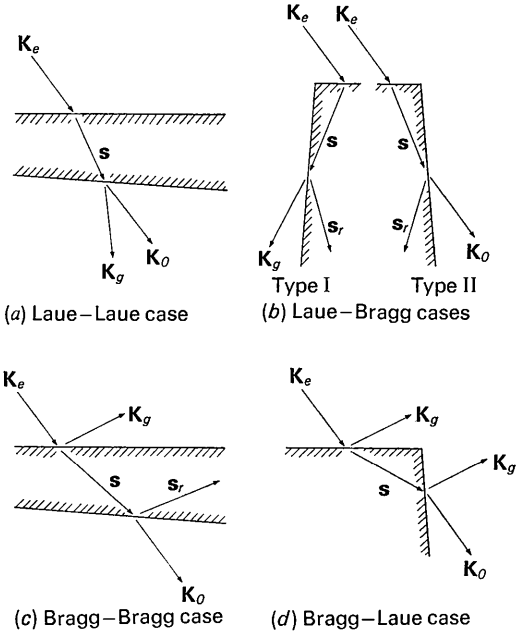

Fig. 1. Schematic illustration of various cases of crystal diffraction.

When a plane wave falls on the crystal surface from the vacuum side, it is obvious that

$$(\mathbf{S}_e \cdot \mathbf{n}_e) > 0 \tag{1}$$

where $\mathbf{n}_e$ is the unit vector of the inward normal of the surface concerned and $\mathbf{S}_e$ is the Poynting vector of the incident wave. For this reason, 'the entrance surface' is defined by equation (1). When the crystal is terminated by another surface and a crystal wave hits this surface, the condition

$$(\mathbf{s} \cdot \mathbf{n}_a) > 0 \tag{2}$$

must be satisfied, where $\mathbf{n}_a$ is the unit outward normal of the surface and $\mathbf{s}$ is the Poynting vector of the crystal wave.* Since the crystal wave is of the Bloch type, the direction of $\mathbf{s}$ must be distinguished from that of the wave vectors $\mathbf{k}_0$ and $\mathbf{k}_g$, particularly when the crystal wave satisfies the Bragg condition to some extent. Hereafter equation (2) will be used as a definition of 'the exit surface'.

In composite crystals including a fault plane, such as stacking fault, twin plane or grain boundary, the fault plane may act as the exit and entrance surfaces for the first and second parts of the crystal respectively. In this case, equation (1) must be read as

$$(\mathbf{s} \cdot \mathbf{n}_e) > 0 \tag{3}$$

for the second part of the crystal. The vector $\mathbf{s}$ in equation (3) is the Poynting vector of the crystal wave in the first part of the crystal.

Next, we shall define the 'Laue and Bragg cases' with respect to the wave vectors. When the Bragg-reflected waves emerge from the entrance surface, we shall call this the 'Bragg case on the entrance surface', whereas when they all propagate through the crystal, the case is called the 'Laue case on the entrance surface'. It is convenient to use the following analytical definitions:

$$\text{Bragg case:} \quad (\bar{\mathbf{K}}_0 \cdot \mathbf{n}_e)(\bar{\mathbf{K}}_g \cdot \mathbf{n}_e) < 0 \tag{4a}$$

$$\text{Laue case:} \quad (\bar{\mathbf{K}}_0 \cdot \mathbf{n}_e)(\bar{\mathbf{K}}_g \cdot \mathbf{n}_e) > 0 \tag{4b}$$

where $\bar{\mathbf{K}}_0$ and $\bar{\mathbf{K}}_g$ are the wave vectors of the incident and Bragg-reflected waves respectively, which satisfy the Bragg condition exactly in a kinematical sense. By the definition (1), $(\bar{\mathbf{K}}_0 \cdot \mathbf{n}_e)$ is always positive so that the definitions (4*a* and *b*) are essentially referred to the sign of $(\bar{\mathbf{K}}_g \cdot \mathbf{n}_e)$.

On the exit surface, if it exists, the definitions can be given similarly as follows;

$$\text{Bragg case:} \quad (\bar{\mathbf{K}}_0 \cdot \mathbf{n}_a)(\bar{\mathbf{K}}_g \cdot \mathbf{n}_a) < 0 \tag{5a}$$

$$\text{Laue case:} \quad (\bar{\mathbf{K}}_0 \cdot \mathbf{n}_a)(\bar{\mathbf{K}}_g \cdot \mathbf{n}_a) > 0 \tag{5b}$$

* Throughout this paper, quantities pertinent to vacuum and crystal media are distinguished by capital and small letters, respectively.

Since the Poynting vector **s** is a weighted mean of the wave vectors $\bar{\mathbf{K}}_0$ and $\bar{\mathbf{K}}_g$ to a good approximation, and as a result of definition (2), both $(\bar{\mathbf{K}}_0 \cdot \mathbf{n}_a)$ and $(\bar{\mathbf{K}}_g \cdot \mathbf{n}_a)$ are positive in the Laue case. It is clear, therefore, that *O* and *G* waves penetrate through the exit surface. In the Bragg case, only one of *O* and *G* waves can pass through the surface. In this case one can assign a definite sign neither to $(\bar{\mathbf{K}}_0 \cdot \mathbf{n}_a)$ nor to $(\bar{\mathbf{K}}_g \cdot \mathbf{n}_a)$.

Since we need to consider at least a pair of entrance and exit surfaces, it is appropriate to specify the geometrical situation of the Bragg reflexion by four cases; Laue–Laue, Laue–Bragg, Bragg–Bragg and Bragg–Laue. Fig. 1 shows these cases schematically. Here, contrary to the conventional usage, the term the 'Laue or Bragg case' is used only for a single surface. In more general cases, when a Bloch wave is reflected *m* times in succession at the crystal surfaces, one needs a more detailed specification such as Laue–(Bragg)^m. If vacuum waves are created by the Laue–(Bragg)^m wave under the Laue condition, they are called the Laue–(Bragg)^m–Laue waves.

The Laue-Bragg case: plane-wave theory

According to the dynamical theory of crystal diffraction, under the two-beam approximation, an incident wave excites two Bloch waves, (1) and (2), in a crystal. Each Bloch wave is composed of two component waves, the direct and the Bragg-reflected waves. For an incident wave of the form $E_e \exp[i(\mathbf{K}_e \cdot \mathbf{r})]$, they are represented in the following form (Zachariasen, 1945; Kato, 1961*a*).

The direct wave:

$$d_0(\mathbf{r}) = E_e C_0 \exp[i\{(\mathbf{K}_e \cdot \mathbf{r}_e) + [\mathbf{k}_0 \cdot (\mathbf{r} - \mathbf{r}_e)]\}] . \quad (6a)$$

The Bragg-reflected wave:

$$d_g(\mathbf{r}) = E_e C_g \exp[i\{[(\mathbf{K}_e + 2\pi\mathbf{g}) \cdot \mathbf{r}_e] + [\mathbf{k}_g \cdot (\mathbf{r} - \mathbf{r}_e)]\}] \quad (6b)$$

where C_0 and C_g are the amplitude factors and $\mathbf{r}_e$ indicates the position vector on the entrance surface. Meanwhile, the indices (1) and (2) specifying the types of Bloch waves are omitted in d_0, C_0 and $\mathbf{k}_0$ and d_g, C_g and $\mathbf{k}_g$.* The wave vectors $\mathbf{k}_0$ and $\mathbf{k}_g$ are related to $\mathbf{K}_e$ as follows (Laue, 1960),

$$\mathbf{k}_0 = \mathbf{K}_e - K\delta_e \mathbf{n}_e \quad \text{(tangential continuity)} \quad (7)$$

$$\mathbf{k}_g = \mathbf{k}_0 + 2\pi\mathbf{g} \quad \text{(reflexion condition)}. \quad (8)$$

The amplitude factors C_0 and C_g, and the 'Anpassung' δ_e, are functions of a reflexion strength β and a parameter *s* specifying the departure from the exact Bragg condition. The analytical expressions are listed in Tables 1 and 2. The definitions of β and *s* are as follows,

$$\beta = KC(\chi_g \chi_{-g})^{\frac{1}{2}} \left(\frac{\gamma_g}{\gamma_0}\right)^{\frac{1}{2}} \frac{1}{\sin 2\theta_B} \equiv \left(\frac{\gamma_g}{\gamma_0}\right)^{\frac{1}{2}} \beta_g \quad (9)$$

$$s = -K_x + \frac{K\chi_0}{2\sin 2\theta_B}\left(1 - \frac{\gamma_g}{\gamma_0}\right) . \quad (10)$$

In these formulae, θ_B is the Bragg angle, *C* the polarization factor and *K* and K_x the magnitude and *x*-component of $\mathbf{K}_e$; the coordinate axes are shown in Fig. 2. The quantities χ_0 and χ_g are the zeroth and *g*-th Fourier coefficients respectively of the polarizability of the crystal for X-rays and γ_0 and γ_g are $(\hat{\mathbf{K}}_0 \cdot \mathbf{n}_e)$ and $(\hat{\mathbf{K}}_g \cdot \mathbf{n}_e)$ respectively.†

By inserting equations (7) and (8) into equations (6*a*) and (6*b*), $d_0(\mathbf{r})$ and $d_g(\mathbf{r})$ can be rewritten as follows,

$$d_0(\mathbf{r}) = E_e C_0 A_0 \exp[i\{\pm\xi_1\sqrt{s^2+\beta^2} - \xi_2 s\}] \quad (11a)$$

$$d_g(\mathbf{r}) = E_e C_g A_g \exp[i\{\pm\xi_1\sqrt{s^2+\beta^2} - \xi_2 s\}] . \quad (11b)$$

The quantities ξ_1 and ξ_2 are functions of position parameters *x* and *t*, the latter being the depth of the observation point from the entrance surface, defined by

$$t = [(\mathbf{r} - \mathbf{r}_e) \cdot \mathbf{n}_e] . \quad (12)$$

* Here, Bloch wave (1) belongs to the branch of the dispersion surface which is closer to the Lorentz point.

† ˆ indicates a unit vector.

Table 1. *The explicit forms of the amplitude factors* $\{C\}$

The Laue case

C_0	$\frac{1}{2}(-s \pm \sqrt{s^2+\beta^2})/(\pm\sqrt{s^2+\beta^2})$
C_g	$\pm\frac{1}{2}(\chi_g/\chi_{-g})^{1/2}(\gamma_0/\gamma_g)^{1/2}\beta/\sqrt{s^2+\beta^2}$

The Laue–Bragg cases

	Type I	Type II
$C_{0,r}$	$-\frac{1}{2}(-s \pm \sqrt{s^2+\beta^2})/(\pm\sqrt{s^2+\beta^2})$	$\frac{1}{2}(\gamma_0/\gamma_g)\,(\gamma_g''/\gamma_0'')\,(s \pm \sqrt{s^2+\beta^2})/(\pm\sqrt{s^2+\beta^2})$
$C_{g,r}$	$\frac{1}{2}\left(\frac{\chi_g}{\chi_{-g}}\right)^{1/2}\left(\frac{\gamma_g'}{\gamma_0'}\right)^{1/2}\frac{\gamma_0}{\gamma_g}\frac{(-s \pm \sqrt{s^2+\beta^2})^2}{(\pm\beta\sqrt{s^2+\beta^2})}$	$-\frac{1}{2}\left(\frac{\chi_g}{\chi_{-g}}\right)^{1/2}\left(\frac{\gamma_0}{\gamma_g}\right)^{1/2}\frac{\beta}{(\pm\sqrt{s^2+\beta^2})}$
$C_{g,t}$	$\pm\frac{1}{2}\left(\frac{\chi_g}{\chi_{-g}}\right)^{1/2}\left\{\left(\frac{\gamma_0}{\gamma_g}\right)^{1/2}\frac{\beta}{\sqrt{s^2+\beta^2}} + \left(\frac{\gamma_g}{\gamma_0}\right)^{1/2}\frac{\gamma_0'}{\gamma_g'}\frac{(-s \pm \sqrt{s^2+\beta^2})^2}{\beta\sqrt{s^2+\beta^2}}\right\}$	
$C_{0,t}$		$\pm\frac{1}{2}\left\{\frac{-s \pm \sqrt{s^2+\beta^2}}{\sqrt{s^2+\beta^2}} + \frac{\gamma_0}{\gamma_g}\frac{\gamma_g''}{\gamma_0''}\frac{s \pm \sqrt{s^2+\beta^2}}{\sqrt{s^2+\beta^2}}\right\}$

The explicit forms of ξ_1 and ξ_2 are given in Table 3. The factors A_0 and A_g are given by

$$A_0=\exp[i(P+K_y y+K_z z)] \tag{13a}$$
$$A_g=A_0\exp[2\pi i(\mathbf{g}\,.\,\mathbf{r})] \tag{13b}$$

where K_y and K_z are the y and z components of $\mathbf{K}_e$ and P is the phase independent of the parameter s,

$$P=\frac{K\chi_0}{2\gamma_0}t-\frac{K\chi_0}{2\sin 2\theta_B}\left(\frac{\gamma_g}{\gamma_0}-1\right)x\,. \tag{14}$$

For later purposes, the 'Resonanzfehler' $\Delta\eta_0$ and $\Delta\eta_g$ are introduced as

$$\Delta\eta_0=[\hat{\bar{\mathbf{K}}}_0\,.\,(\mathbf{k}_0-\bar{\mathbf{k}}_0)] \tag{15a}$$
$$\Delta\eta_g=[\hat{\bar{\mathbf{K}}}_g\,.\,(\mathbf{k}_g-\bar{\mathbf{k}}_g)] \tag{15b}$$

where $\bar{\mathbf{k}}_0$ and $\bar{\mathbf{k}}_g$ are the wave vectors $\vec{LO}$ and $\vec{LG}$ in Fig. 2. The 'Resonanzfehler' are determined by the dispersion relation

$$\Delta\eta_0\,.\,\Delta\eta_g=\tfrac{1}{4}K^2C^2\chi_g\chi_{-g}\,. \tag{16}$$

They are represented in terms of the parameter s and listed in Table 4.

So far, we have considered the crystal waves excited on the entrance surface. Now, the reflexion and transmission of the waves on the exit surface are considered. We must distinguish two modes of reflexion, Type I and Type II [see Fig. 1(*b*)]. In the former, $(\bar{\mathbf{K}}_0\,.\,\mathbf{n}_a)$ is negative and in the latter $(\bar{\mathbf{K}}_g\,.\,\mathbf{n}_a)$ is negative. Consequently, either the O wave or the G wave is totally reflected at the exit surface according to the prevailing mode.

(*a*) *Type* I

The boundary conditions at the exit surface are given by

$$E_{g,t}\exp[i(\mathbf{K}_{g,t}\,.\,\mathbf{r}_a)]=d_g\exp[i(\mathbf{k}_g\,.\,\mathbf{r}_a)]+d_{g,r}\exp[i(\mathbf{k}_{g,r}\,.\,\mathbf{r}_a)] \tag{17a}$$

$$0=d_0\exp[i(\mathbf{k}_0\,.\,\mathbf{r}_a)]+d_{0,r}\exp[i(\mathbf{k}_{0,r}\,.\,\mathbf{r}_a)] \tag{17b}$$

where the subscripts r and t are used for the quantities corresponding to the reflected and transmitted wave fields, and $\mathbf{r}_a$ indicates a point on the exit surface. $E_{g,t}$ and $\mathbf{K}_{g,t}$ are the amplitude* and the wave vector of the vacuum wave respectively. From the tangential continuity condition, the wave vectors must satisfy the relations,

$$\mathbf{k}_{0,r}=\mathbf{k}_0+K\delta_r\mathbf{n}_a \tag{18a}$$
$$\mathbf{k}_{g,r}=\mathbf{k}_g+K\delta_r\mathbf{n}_a \tag{18b}$$
$$\mathbf{K}_{g,t}=\mathbf{k}_g+K\delta_g\mathbf{n}_a\,. \tag{18c}$$

The condition of Bragg reflexion for the reflected waves

$$\mathbf{k}_{g,r}=\mathbf{k}_{0,r}+2\pi\mathbf{g} \tag{19}$$

is assured by taking the same Anpassung for the O and G waves.

By using equations (7) and (8) and the relation $\mathbf{K}_e+2\pi\mathbf{g}=\bar{\mathbf{K}}_g+\mathbf{K}_x$, equation (18*c*) is rewritten as,

$$\mathbf{K}_{g,t}=(\bar{\mathbf{K}}_g+\mathbf{K}_x)-K\delta_e\mathbf{n}_e+K\delta_g\mathbf{n}_a\,. \tag{20}$$

The Anpassung δ_g is easily obtained, by taking the scalar product of equation (20) with $\bar{\mathbf{K}}_g$ and using the approximation $(\mathbf{K}_{g,t}\,.\,\bar{\mathbf{K}}_g)=K^2$, giving

$$K\delta_g=-\frac{\sin 2\theta_B}{\gamma_g'}K_x+\frac{\gamma_g}{\gamma_g'}K\delta_e \tag{21}$$

where γ_g' is defined by equation (24*b*) below.

To evaluate the Anpassung δ_r, it is convenient to introduce again the Resonanzfehler, $\Delta\eta_{0,r}$ and $\Delta\eta_{g,r}$, for the reflected Bloch wave. These are defined by

$$\Delta\eta_{0,r}=[\hat{\bar{\mathbf{K}}}_0\,.\,(\mathbf{k}_{0,r}-\bar{\mathbf{k}}_0)] \tag{22a}$$
$$\Delta\eta_{g,r}=[\hat{\bar{\mathbf{K}}}_g\,.\,(\mathbf{k}_{g,r}-\bar{\mathbf{k}}_g)]\,. \tag{22b}$$

By inserting equations (18*a* and *b*) into equations (22*a*

* To save letters, the amplitude and the wave field are expressed in the same notation, the latter being accompanied by the variable **r**.

Table 2. *The explicit forms of the Anpassungen* $\{\delta\}$

$\alpha=\sin 2\theta_B/(2\gamma_g)$.

The Laue case

$K\delta_e$ $\quad -\frac{1}{2}K\chi_0/\gamma_0-\alpha(s\pm\sqrt{s^2+\beta^2})$

The Laue–Bragg cases

	Type I	Type II
$K\delta_r$	$-\alpha\left(\frac{\gamma_0}{\gamma_0'}-\frac{\gamma_g}{\gamma_g'}\right)s\mp\alpha\left(\frac{\gamma_0}{\gamma_0'}+\frac{\gamma_g}{\gamma_g'}\right)\sqrt{s^2+\beta^2}$	$-\alpha\left(\frac{\gamma_0}{\gamma_0''}-\frac{\gamma_g}{\gamma_g''}\right)s\mp\alpha\left(\frac{\gamma_0}{\gamma_0''}+\frac{\gamma_g}{\gamma_g''}\right)\sqrt{s^2+\beta^2}$
$K\delta_g$	$-\frac{1}{2}\frac{K\chi_0}{\gamma_g'}+\alpha\frac{\gamma_g}{\gamma_g'}(s\mp\sqrt{s^2+\beta^2})$	
$K\delta_0$		$-\frac{1}{2}\frac{K\chi_0}{\gamma_0''}-\alpha\frac{\gamma_0}{\gamma_0''}(s\pm\sqrt{s^2+\beta^2})$

and *b*) and taking account of the relations (15*a* and *b*), it follows that

$$\Delta\eta_{0,r}=\Delta\eta_0+K\delta_r\gamma_0' \tag{23a}$$

$$\Delta\eta_{g,r}=\Delta\eta_g+K\delta_r\gamma_g' \tag{23b}$$

where

$$\gamma_0'=(\mathring{\mathbf{K}}_0\cdot\mathbf{n}_a) \tag{24a}$$

$$\gamma_g'=(\mathring{\mathbf{K}}_g\cdot\mathbf{n}_a)\,. \tag{24b}$$

Since the dispersion relation holds both for the incident and reflected Bloch waves we shall have

$$\Delta\eta_{0,r}\,.\,\Delta\eta_{g,r}=\Delta\eta_0\,.\,\Delta\eta_g\,. \tag{25}$$

Inserting equations (23*a* and *b*) into this relationship, we can determine the Anpassung and the Resonanzfehler as follows:

$$K\delta_r=-\left(\frac{\Delta\eta_0}{\gamma_0'}+\frac{\Delta\eta_g}{\gamma_g'}\right) \tag{26}$$

$$\Delta\eta_{0,r}=-\frac{\gamma_0'}{\gamma_g'}\Delta\eta_g \tag{27a}$$

$$\Delta\eta_{g,r}=-\frac{\gamma_g'}{\gamma_0'}\Delta\eta_0\,. \tag{27b}$$

Since K_x, δ_e, $\Delta\eta_0$ and $\Delta\eta_g$ have been already obtained as functions of the deviation parameter s, δ_g [equation (21)] and δ_r [equation (26)] and $\Delta\eta_{0,r}$ and $\Delta\eta_{g,r}$ [equations (27)] can be expressed in terms of s. The results are shown in Tables 2 and 4.

The amplitude ratio of O and G waves for the reflected Bloch wave depends on the Resonanzfehler, as in the case of the incident Bloch wave, in the form

$$c_r\equiv\frac{d_{g,r}}{d_{0,r}}=\frac{KC\chi_g}{2\Delta\eta_{g,r}}=\frac{2\Delta\eta_{0,r}}{KC\chi_{-g}}\,. \tag{28}$$

Introducing this ratio into equations (17*a* and *b*), and writing the wave fields in the following forms,

$$d_{0,r}(\mathbf{r})=E_eC_{0,r}\exp\,[i\{(\mathbf{K}_e\,.\,\mathbf{r}_e)+[\mathbf{k}_0\,.\,(\mathbf{r}_a-\mathbf{r}_e)]+[\mathbf{k}_{0,r}\,.\,(\mathbf{r}-\mathbf{r}_a)]\}] \tag{29a}$$

$$d_{g,r}(\mathbf{r})=E_eC_{g,r}\exp\,[i\{[(\mathbf{K}_e+2\pi\mathbf{g})\,.\,\mathbf{r}_e]+[\mathbf{k}_g\,.\,(\mathbf{r}_a-\mathbf{r}_e)]+[\mathbf{k}_{g,r}\,.\,(\mathbf{r}-\mathbf{r}_a)]\}] \tag{29b}$$

$$E_{g,t}(\mathbf{r})=E_eC_{g,t}\exp\,[i\{[(\mathbf{K}_e+2\pi\mathbf{g})\,.\,\mathbf{r}_e]+[\mathbf{k}_g\,.\,(\mathbf{r}_a-\mathbf{r}_e)]+[\mathbf{K}_{g,t}\,.\,(\mathbf{r}-\mathbf{r}_a)]\}] \tag{29c}$$

we have

$$C_{0,r}=-C_0 \tag{30a}$$

$$C_{g,r}=c_rC_{0,r} \tag{30b}$$

$$C_{g,t}=C_g+C_{g,r}\,. \tag{30c}$$

In the same way as in the case of equations (11*a* and *b*), the wave fields, equations (29), can be rewitten as

$$d_{0,r}(\mathbf{r})=E_eC_{0,r}A_0\exp\,[i\{\pm\eta_1\sqrt{s^2+\beta^2}-\eta_2 s\}] \tag{31a}$$

$$d_{g,r}(\mathbf{r})=E_eC_{g,r}A_g\exp\,[i\{\pm\eta_1\sqrt{s^2+\beta^2}-\eta_2 s\}] \tag{31b}$$

$$E_{g,t}(\mathbf{r})=E_eC_{g,t}A_{g,t}\exp\,[i\{\pm\zeta_1\sqrt{s^2+\beta^2}-\zeta_2 s\}] \tag{31c}$$

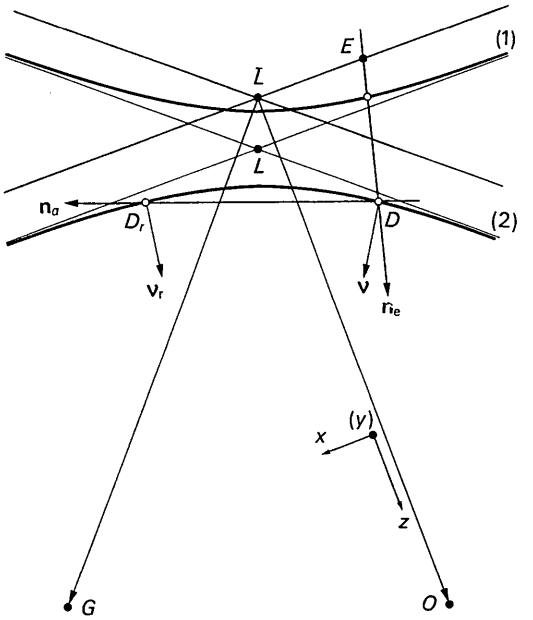

Fig. 2. The dispersion surface and the construction of dispersion points (Laue–Bragg cases; Type I). L: Lorentz point. L: Laue point. $\vec{LO}=\bar{\mathbf{K}}_0$, $\vec{LG}=\bar{\mathbf{K}}_g$, $\vec{LO}=\bar{\mathbf{k}}_0$ and $\vec{LG}=\bar{\mathbf{k}}_g$. Normals $\mathbf{n}_e$ and $\mathbf{n}_a$ do not necessarily lie on the plane of drawing which is determined by $\mathbf{K}_e=\vec{EO}$ and $2\pi\mathbf{g}=\vec{OG}$.

Table 3. *The explicit forms of* ξ_i, η_i *and* ζ_i $(i=1,2)$

The Laue case

ξ_1	αt
ξ_2	$x-\alpha t$

The Laue–Bragg cases

	Type I	Type II
η_1	$\alpha t-\alpha t_a\{(\gamma_0/\gamma_0')+(\gamma_g/\gamma_g')\}$	$\alpha t-\alpha t_b\{(\gamma_0/\gamma_0'')+(\gamma_g/\gamma_g'')\}$
η_2	$x-\alpha t+\alpha t_a\{(\gamma_0/\gamma_0')-(\gamma_g/\gamma_g')\}$	$x-\alpha t+\alpha t_b\{(\gamma_0/\gamma_0'')-(\gamma_g/\gamma_g'')\}$
ζ_1	$\alpha t-\alpha t_a(\gamma_g/\gamma_g')$	$\alpha t-\alpha t_b(\gamma_0/\gamma_0'')$
ζ_2	$x-\alpha t-\alpha t_a(\gamma_g/\gamma_g')$	$x-\alpha t+\alpha t_b(\gamma_0/\gamma_0'')$

where A_0 and A_g are given by equations (13*a* and *b*). The factor $A_{g,t}$ is given by

$$A_{g,t}=A_g \exp\left(-i\frac{K\chi_0}{2\gamma'_g}t_a\right) \tag{32}$$

where
$$t_a=(\mathbf{r}-\mathbf{r}_a)\cdot\mathbf{n}_a \tag{33}$$

means the depth of the position vector from the exit surface. It is to be noticed that t_a is positive when $\mathbf{r}$ is in vacuum, and negative in the crystal. Sometimes, we use the notation

$$P_g=P-\frac{K\chi_0}{2\gamma'_g}t_a\,. \tag{34}$$

The amplitude factors $C_{0,r}$, $C_{g,r}$ and $C_{g,t}$ are expressed in terms of s and the results are shown in Table 1. The quantities η_1, η_2, ζ_1 and ζ_2 are functions of position parameters x, t and t_a and shown in Table 3.

(*b*) *Type* II

In this case, the G component of the incident Bloch wave is totally reflected. The wave fields can be obtained by similar procedures to those used in Type I. The boundary conditions are read as

$$E_{0,t}\exp[i(\mathbf{K}_{0,t}\cdot\mathbf{r}_b)]=d_0\exp[i(\mathbf{k}_0\cdot\mathbf{r}_b)]+d_{0,r}\exp[i(\mathbf{k}_{0,r}\cdot\mathbf{r}_b)] \tag{35a}$$

$$0=d_g\exp[i(\mathbf{k}_g\cdot\mathbf{r}_b)]+d_{g,r}\exp[i(\mathbf{k}_{g,r}\cdot\mathbf{r}_b)] \tag{35b}$$

where $E_{0,t}$ and $\mathbf{K}_{0,t}$ are the amplitude and the wave vector of the transmitted vacuum wave, and $\mathbf{r}_b$ indicates a point on the exit surface.

The Anpassung of the wave vectors of the reflected crystal waves, corresponding to equation (26), is given by

$$K\delta_r=-\left(\frac{\Delta\eta_0}{\gamma''_0}+\frac{\Delta\eta_g}{\gamma''_g}\right) \tag{36}$$

where

$$\gamma''_0=(\mathring{\mathbf{K}}_0\cdot\mathbf{n}_b) \tag{37a}$$

$$\gamma''_g=(\mathring{\mathbf{K}}_g\cdot\mathbf{n}_b) \tag{37b}$$

$\mathbf{n}_b$ being the outward normal of the exit surface. Similarly, the Anpassung of the wave vector of the transmitted vacuum wave is obtained as

$$K\delta_0=\frac{\gamma_0}{\gamma''_0}K\delta_e \tag{38}$$

which corresponds to equation (21). The expressions (27*a* and *b*) of the Resonanzfehler and the amplitude ratio, equation (28), need not to be altered provided that γ'_0 and γ'_g are replaced by γ''_0 and γ''_g respectively. The explicit forms of the Anpassungen δ_r and δ_0 and the Resonanzfehler are shown in Tables 2 and 4.

Writing the wave fields in a similar form to that of equations (29), as

$$d_{0,r}(\mathbf{r})=E_eC_{0,r}\exp[i\{(\mathbf{K}_e\cdot\mathbf{r}_e)+[\mathbf{k}_0\cdot(\mathbf{r}_b-\mathbf{r}_e)]+[\mathbf{k}_{0,r}\cdot(\mathbf{r}-\mathbf{r}_b)]\}] \tag{39a}$$

$$d_{g,r}(\mathbf{r}_g)=E_eC_{,r}\exp[i\{[(\mathbf{K}_e+2\pi\mathbf{g})\cdot\mathbf{r}_e]+[\mathbf{k}_g\cdot(\mathbf{r}_b-\mathbf{r}_e)]+[\mathbf{k}_{g,r}\cdot(\mathbf{r}-\mathbf{r}_b)]\}] \tag{39b}$$

$$E_{0,t}(\mathbf{r})=E_eC_{0,t}\exp[i\{(\mathbf{K}_e\cdot\mathbf{r}_e)+[\mathbf{k}_0\cdot(\mathbf{r}_b-\mathbf{r}_e)]+[\mathbf{K}_{0,t}\cdot(\mathbf{r}-\mathbf{r}_b)]\}] \tag{39c}$$

we obtain the amplitude factors as follows,

$$C_{0,r}=\frac{1}{c_r}C_{g,r} \tag{40a}$$

$$C_{g,r}=-C_g \tag{40b}$$

$$C_{0,t}=C_0+C_{0,r}\,. \tag{40c}$$

By the same procedures as those employed in Type I, the wave fields can be expressed as,

$$d_{0,r}(\mathbf{r})=E_eC_{0,r}A_0\exp[i\{\pm\eta_1\sqrt{s^2+\beta^2}-\eta_2 s\}] \tag{41a}$$

$$d_{g,r}(\mathbf{r})=E_eC_{g,r}A_g\exp[i\{\pm\eta_1\sqrt{s^2+\beta^2}-\eta_2 s\}] \tag{41b}$$

$$E_{0,t}(\mathbf{r})=E_eC_{0,t}A_{0,t}\exp[i\{\pm\zeta_1\sqrt{s^2+\beta^2}-\zeta_2 s\}] \tag{41c}$$

where A_0 and A_g are given by equations (13*a* and *b*). The factor $A_{0,t}$ is given by

$$A_{0,t}=A_0\exp\left(-i\frac{K\chi_0}{2\gamma''_0}t_b\right) \tag{42}$$

where
$$t_b=[(\mathbf{r}-\mathbf{r}_b)\cdot\mathbf{n}_b] \tag{43}$$

means the depth from the exit surface. Again, t_b is positive when $\mathbf{r}$ is in vacuum and negative in the crystal. Corresponding to equation (34), it is convenient to introduce the notation

$$P_0=P-\frac{K\chi_0}{2\gamma''_0}t_b\,. \tag{44}$$

The explicit forms of $C_{0,r}$, $C_{g,r}$ and $C_{0,t}$ and η_1, η_2, ζ_1 and ζ_2 are shown in Tables 1 and 3.

The Laue-Bragg case: spherical-wave theory

Under the usual conditions of X-ray diffraction experiments, an incident wave has to be regarded as a spherical wave. Consequently, there exists a triangular fan of wave fields between the directions of $\bar{\mathbf{K}}_0$ and $\bar{\mathbf{K}}_g$ passing through the entrance point. In this section a spherical-wave theory is developed based on the plane-wave theory described in the previous section. The procedures are similar to the spherical-wave theory in the Laue case for crystals including a stacking fault (Kato, Usami & Katagawa, 1967).

A spherical wave can be represented by a Fourier integral or a superposition of plane waves as follows,

$$\Phi\equiv\frac{e^{iKr}}{4\pi r}=\frac{i}{8\pi^2}\int\!\!\int\frac{\exp[i(\mathbf{K}\cdot\mathbf{r})]}{K_z}\mathrm{d}K_x\mathrm{d}K_y\,. \tag{45}$$

On the entrance surface, this wave excites the O and G component waves, which have been given in previous

papers (Kato, 1961*b*, 1968). These are reflected at the exit surface. The descriptions are given for Type I and II separately, as in the previous section.

(*a*) *Type* I

We shall take the incident wave having the form of $E_e\Phi$, where Φ is given by equation (45). Since a plane wave $E_e \exp i(\mathbf{K}\,.\,\mathbf{r})$ produces the reflected wave fields $d_{0,r}(\mathbf{r})$ and $d_{g,r}(\mathbf{r})$, which are given by equations (31*a* and *b*), the corresponding waves excited by the spherical wave $E_e\Phi$ can be represented in the forms,

O waves:

$$\phi_{0,r}(\mathbf{r}) = \frac{i}{8\pi^2}\int\int_{-\infty}^{+\infty} \frac{d_{0,r}(\mathbf{r})}{K_z}\,\mathrm{d}K_x\mathrm{d}K_y\,. \qquad (46a)$$

G waves:

$$\phi_{g,r}(\mathbf{r}) = \frac{i}{8\pi^2}\int\int_{-\infty}^{+\infty} \frac{d_{g,r}(\mathbf{r})}{K_z}\,\mathrm{d}K_x\mathrm{d}K_y\,. \qquad (46b)$$

The integration with respect to K_y can be carried out by the stationary phase method. This results in a multiplication factor $D_y = \sqrt{2\pi K/z}\,\exp(-i\pi/4)$. By virtue of the expressions for $d_{0,r}(\mathbf{r})$ and $d_{g,r}(\mathbf{r})$, $\phi_{0,r}(\mathbf{r})$ and $\phi_{g,r}(\mathbf{r})$ can be written explicitly in terms of the parameter s.

$$\phi_{0,r}(\mathbf{r}) = -\tfrac{1}{2}[U_0(+)+U_0(-)]\,.\,B_0E_e \qquad (47a)$$

$$\phi_{g,r}(\mathbf{r}) = \tfrac{1}{2}\left(\frac{\chi_g}{\chi_{-g}}\right)^{\pm}\left(\frac{\gamma_g}{\gamma_0}\right)^{\pm}\frac{\gamma_0'}{\gamma_g'}[U_g(+) + U_g(-)]\,.\,B_gE_e \qquad (47b)$$

where

$$B_0 = \frac{i}{8\pi^2}\sqrt{\frac{2\pi}{Kz}}\exp\left[i\left(-\frac{\pi}{4}+P+Kz\right)\right] \qquad (48a)$$

$$B_g = B_0\exp[2\pi i(\mathbf{g}\,.\,\mathbf{r})] \qquad (48b)$$

$$U_0(\pm) = \int_{-\infty}^{+\infty} \frac{-s\pm\sqrt{s^2+\beta^2}}{\pm\sqrt{s^2+\beta^2}}\exp[i(\pm\eta_1\sqrt{s^2+\beta^2}-\eta_2 s)]\mathrm{d}s^r \qquad (49a)$$

$$U_g(\pm) = \int_{-\infty}^{+\infty} \frac{(-s\pm\sqrt{s^2+\beta^2})^2}{\beta(\pm\sqrt{s^2+\beta^2})}\exp[i(\pm\eta_1\sqrt{s^2+\beta^2}-\eta_2 s)]\mathrm{d}s^r. \qquad (49b)$$

The integrations can be performed straightforwardly as shown in Appendix *A*, s^r being the real part of s. As is seen there, only $\eta_1 \pm \eta_2$ appear in the spherical-wave solutions. They are represented in terms of $x_{0,r}$ and $x_{g,r}$, which are the normal distances from the observation point P to the lines JF_aJ' and LF_aL' in Fig. 3(*a*). The intersection F_a is constructed as follows. The lines passing through the entrance point E in the directions $\bar{\mathbf{K}}_g$ and $\bar{\mathbf{K}}_0$ intersect with the exit surface S_a and its extension S_a^* at $\bar{A}$ and $\bar{A}^*$ respectively. The point F_a is the intersection of the lines passing through $\bar{A}$ and $\bar{A}^*$ in the directions of $\bar{\mathbf{K}}_0$ and $\bar{\mathbf{K}}_g$ respectively. The expressions for $\eta_1 \pm \eta_2$ are given in Appendix *B*, [equations (*B*8*a* and *b*)]. The wave fields, then, have the forms,

$$\phi_{0,r}(\mathbf{r}) = \pi\beta_g\frac{\gamma_g'}{|\gamma_0'|}\sqrt{\frac{x_{0,r}}{x_{g,r}}}\,J_1(\beta_g\sqrt{x_{0,r}x_{g,r}})\,.\,B_0E_e \quad \text{for } x_{0,r}x_{g,r}>0;\quad =0 \quad \text{for } x_{0,r}x_{g,r}<0 \qquad (50a)$$

$$\phi_{g,r}(\mathbf{r}) = i\pi\beta_g\left(\frac{\chi_g}{\chi_{-g}}\right)^{\pm}\frac{\gamma_g'}{|\gamma_0'|}\,\mathrm{sign}\,(x_{0,r})\,\frac{x_{0,r}}{x_{g,r}} \times J_2(\beta_g\sqrt{x_{0,r}x_{g,r}})\,.\,B_gE_e \quad \text{for } x_{0,r}x_{g,r}>0;\quad =0 \quad \text{for } x_{0,r}x_{g,r}<0 \qquad (50b)$$

where J_n is the Bessel function of order n, and β_g has been defined by equation (9). The wave fields (50*a* and *b*), therefore, take non-zero values only within the hatched regions [Fig. 3(*a*)]. They have the forms very similar to the wave fields in the Laue case, the point F_a playing the role of the point E in the Laue case.

The result can be interpreted by considering the rays associated with the plane-wave solution. The ray directions of the wave fields represented by Fourier integrals like equations (49*a* and *b*) can be obtained by the stationary phase method as in the treatment of Kato, Usami & Katagawa (1967). The stationary condition of the phase reads

$$-\eta_2 \pm \frac{s}{\sqrt{s^2+\beta^2}}\eta_1 = 0\,. \qquad (51)$$

This implies that all rays are straight lines, the direction being specified by s. For sufficiently large values of

Table 4. *The explicit forms of the Resonanzfehler* $\{\Delta\eta\}$

The Laue case

$\Delta\eta_0$	$\alpha\gamma_0(s\pm\sqrt{s^2+\beta^2})$
$\Delta\eta_g$	$\alpha\gamma_g(-s\pm\sqrt{s^2+\beta^2})$

The Laue–Bragg cases

	Type I	Type I
$\Delta\eta_{0,r}$	$-\alpha\gamma_g(\gamma_0'/\gamma_g')\,(-s\pm\sqrt{s^2+\beta^2})$	$-\alpha\gamma_g(\gamma_0''/\gamma_g'')\,(-s\pm\sqrt{s^2+\beta^2})$
$\Delta\eta_{g,r}$	$-\alpha\gamma_0(\gamma_g'/\gamma_0')\,(s\pm\sqrt{s^2+\beta^2})$	$-\alpha\gamma_0(\gamma_g''/\gamma_0'')\,(s\pm\sqrt{s^2+\beta^2})$

$|s|$, equation (51) tends to $\eta_1 \pm \eta_2 = 0$, namely lines LL' and JJ'. The intersection $\eta_1 = \eta_2 = 0$, therefore, is the point F_a explained above. Since equation (51) holds irrespective of the value of s for $\eta_1 = 0$ and $\eta_2 = 0$, all rays pass through the point F_a.

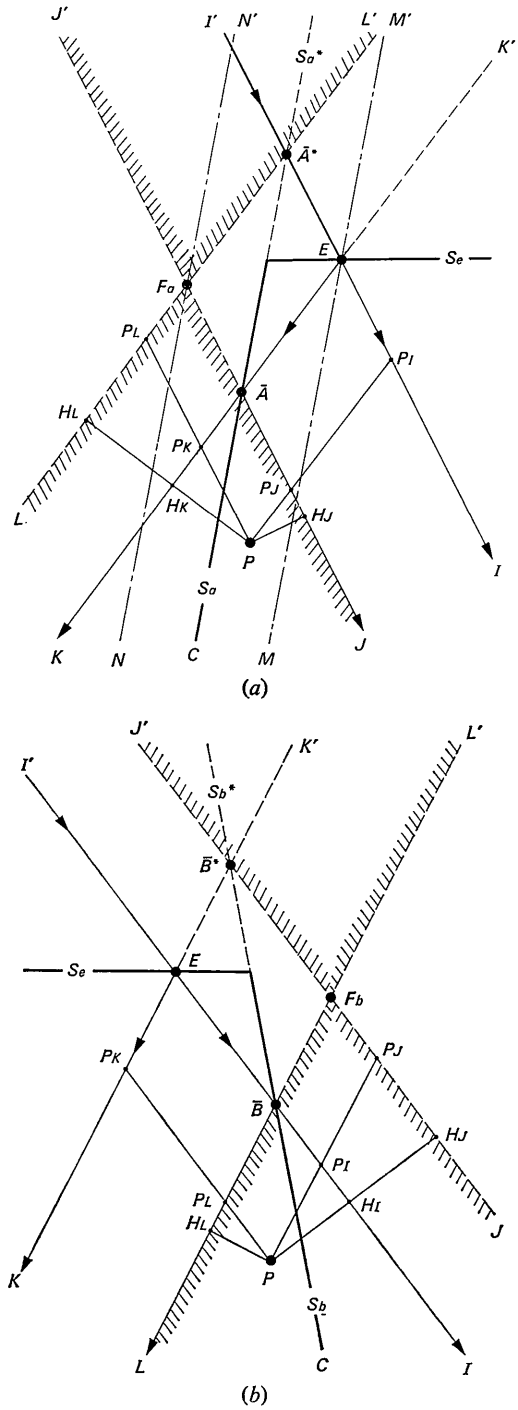

Fig. 3. The Laue–Bragg cases. (*a*) Type I, (*b*) Type II. S_e: The entrance surface. S_a and S_b: exit surfaces. P: Observation point. $P_K P = l_0$, $P_I P = l_g$, $P_L P = l_{0,r}$, $P_J P = l_{g,r}$, $H_I P = x_0$, $H_K P = x_g$, $H_J P = x_{0,r}$, $H_L P = x_{g,r}$.

Physically speaking, the rays created at E in the directions between EK and EM are really reflected at the exit surface S_a. The rays propagating in the directions between EM and EI are imaginarily reflected at the hypothetical surface S_a^*. In the wave field obtained in equations (50*a* and *b*), the part between NN' and JJ' is the really reflected wave on the surface S_a and its continuation on the vacuum side, whereas the part between LL' and NN' is nothing more than the imaginarily reflected wave on the surface S_a^*. Since the imaginarily reflected waves do not interfere with the wave field in the triangular fan $C\bar{A}J$, the present solution gives the correct wave field.

(*b*) *Type* II

The wave fields can be obtained in a similar way to the case of Type I. The plane-wave solution, equations (41*a* and *b*) must be inserted in the integrand of equations (46*a* and *b*). The required integrals are calculated in Appendix *A*. The final results are given by

$$\phi_{0,r}(\mathbf{r}) = \pi\beta_g \sqrt{\frac{x_{g,r}}{x_{0,r}}}\, J_1(\beta_g \sqrt{x_{0,r}x_{g,r}})\,.\, B_0 E_e \quad \text{for } x_{0,r}x_{g,r} > 0$$
$$= 0 \quad \text{for } x_{0,r}x_{g,r} < 0 \qquad (52a)$$

$$\phi_{g,r}(\mathbf{r}) = -i\pi\beta_g \left(\frac{\chi_g}{\chi_{-g}}\right)^{\pm} \text{sign}\,(x_{0,r}) \times J_0(\beta_g \sqrt{x_{0,r}x_{g,r}})\,.\, B_g E_e \quad \text{for } x_{0,r}x_{g,r} > 0$$
$$= 0 \quad \text{for } x_{0,r}x_{g,r} < 0 \qquad (52b)$$

where, $x_{0,r}$ and $x_{g,r}$ are the normal distances from the observation point to the lines JJ' and LL' of Fig. 3(*b*). The wave fields take non-zero values only within the hatched regions. They can be interpreted in terms of a bundle of rays. As in the case of Type I, all rays converge at the focal point F_b.

(*c*) *The wave fields penetrating through the exit surface*

The spherical-wave solution can be obtained from the plane-wave solution, equation (31*c*) or (41*c*). The procedure is similar to that used in obtaining the crystal wave fields. The required Fourier integrals are explained in Appendix *A*. The final results are given as follows.

Type I:

$$\Phi_{g,t}(\mathbf{r}) = i\pi\beta_g \left(\frac{\chi_g}{\chi_{-g}}\right)^{\pm} \text{sign}\,(x_g) \times \left\{\frac{x_g}{x_{g,r}} J_2(\beta_g \sqrt{(|\gamma_0'|/\gamma_g')x_g x_{g,r}}) + J_0(\beta_g \sqrt{(|\gamma_0'|/\gamma_g')x_g x_{g,r}})\right\}.\, B_{g,t} E_e \quad \text{for } x_g x_{g,r} > 0$$
$$= 0 \quad \text{for } x_g x_{g,r} < 0\,. \qquad (53a)$$

Type II:

$$\Phi_{0,t}(\mathbf{r})=\pi\beta_g\left(\frac{|\gamma_g''|}{\gamma_0''}\right)^{\pm}\left\{\sqrt{\frac{x_0}{x_{0,r}}}\sqrt{-\frac{x_{0,r}}{x_0}}\right\}\times J_1(\beta_g\sqrt{(|\gamma_g''|/\gamma_0'')x_0x_{0,r}}).\ B_{0,t}E_e \quad \text{for } x_0x_{0,r}>0$$
$$=0 \quad \text{for } x_0x_{0,r}<0 \qquad (53b)$$

where

$$B_{g,t}=\frac{i}{8\pi^2}\sqrt{\frac{2\pi}{Kz}}\exp\left[i\left(-\frac{\pi}{4}+P_g+Kz+2\pi(\mathbf{g}\,.\,\mathbf{r})\right)\right] \qquad (54a)$$

$$B_{0,t}=\frac{i}{8\pi^2}\sqrt{\frac{2\pi}{Kz}}\exp\left[i\left(-\frac{\pi}{4}+P_0+Kz\right)\right]. \qquad (54b)$$

In deriving these, the following relations are used.

$$\left.\begin{aligned}\zeta_1-\zeta_2&=\frac{\gamma_0}{\gamma_g}x_g \qquad (55a)\\ \zeta_1+\zeta_2&=-\frac{\gamma_0'}{\gamma_g'}x_{g,r} \qquad (55b)\end{aligned}\right\}\ \text{Type I}$$

$$\left.\begin{aligned}\zeta_1-\zeta_2&=-\frac{\gamma_0}{\gamma_g}\frac{\gamma_g''}{\gamma_0''}x_{0,r} \qquad (56a)\\ \zeta_1+\zeta_2&=x_0 \qquad (56b)\end{aligned}\right\}\ \text{Type II}$$

where x_g and $x_{g,r}$ are defined in Fig. 3(*a*), and x_0 and $x_{0,r}$ are defined in Fig. 3(*b*). The derivation of these is performed in the same way as in the case of $\eta_1\pm\eta_2$ and is explained in Appendix *B*. Since, from equation (53*a*) the Pendellösung fringes in vacuum are essentially determined only by the quantities x_g and $x_{g,r}$, we know that the fringes are parallel to $\bar{\mathbf{K}}_g$. The same situation is noticeable in the case of Type II, provided that $\bar{\mathbf{K}}_g$ is replaced by $\bar{\mathbf{K}}_0$.

Discussion

In this paper, we have discussed the crystal and vacuum wave fields reflected under the Laue–Bragg conditions. From the view-point of the spherical-wave theory, the crystal wave is composed of *O* and *G* wave fields, which are confined in a triangular fan, emitted from an imaginary focal point F_a or F_b as illustrated in Figs. 3(*a*) and (*b*). As in the Laue case (Kato, 1968), the wave fields are given rigorously by the Fourier transform of the wave fields obtained on the basis of the plane-wave theory.

The results, in relation to some experiments, are discussed in the following paper. Here, only one mathematical aspect, the justification of the integral range s or (K_x) in the spherical-wave theory will be presented.

We shall consider the Laue–Bragg case of Type I. The integral range was assumed to be $(-\infty, +\infty)$ in equations (49*a* and *b*). At first sight, it may seem, from ray considerations, that the integral is taken over superfluous parts of the dispersion surface. In fact, the dispersion points corresponding to $(-\infty, s_0)$ of branch (1) and $(s_0, +\infty)$ of branch (2) denote the waves propagating between the directions *EM* and *EI*, which may seem irrelevant to the reflexions on the surface S_a in Fig. 3(*a*).

To understand this situation, it is worth while considering the plane-wave solutions in the Laue case. Whatever the real crystal shape is, the solutions imply Bloch waves created on the infinitely extended surface S_e and hypothetically conceivable waves on the vacuum side which are continuous with the crystal waves mentioned above. The spherical-wave solution is the superposition of these Bloch waves over all space. Thus, the solution includes the real wave field in the crystal emitted from the entrance point *E* and the imaginary wave field in vacuum converging on the point *E*.

The plane-wave solutions in the Laue–Bragg case are the waves reflected at the surface S_a and its extension S_a^*, as the Bloch waves mentioned in the previous paragraph. They therefore include the waves reflected on the left hand side of S_a and S_a^*, as well as the waves reflected on the right hand side. As in the Laue case, the superposition of such waves, namely the spherical-wave solution, is actually confined within the hatched region in Fig. 3(*a*). The waves corresponding to the apparently superfluous parts of the dispersion surface imply the waves which are reflected on the left side of S_a and S_a^*. On the other hand, the waves corresponding to the physically significant parts imply the waves which are reflected on the right side. From ray considerations, therefore, it can be seen that the rays associated with the latter type of waves, those passing through F_a, amount to the rays actually reflected inside the crystal while the rays associated with the former type of waves are hypothetical ones which are reflected at the extended surface S_a^*. The spherical-wave solution includes this hypothetical part, which does not, however, affect the crystal waves which are actually reflected on the surface S_a, because the hypothetical rays and the real rays are separated in space. For this reason, the mathematical procedure of taking the integral range of s from $-\infty$ to $+\infty$ can be justified in all cases.

APPENDIX *A*

Fourier integrals required for the spherical-wave theory

We shall consider the sum of the integrals

$$U_m=U_m(+)+U_m(-) \qquad (A1)$$

where

$$U_m(\pm)=\left(\frac{1}{\beta}\right)^{m-1}\int_{-\infty}^{+\infty}\frac{(-s\pm\sqrt{s^2+\beta^2})^m}{\pm\sqrt{s^2+\beta^2}}\times\exp\left[i(\pm\eta_1\sqrt{s^2+\beta^2}-\eta_2 s)\right]ds^r. \qquad (A2)$$

These integrals always appear in the case of Type I, not only for the Laue–Bragg case but also for the Laue–

(Bragg)^m cases which will be explained in the next paper. In the Laue–Bragg case, the values $m=1$ (O wave) and $m=2$ (G wave) are used.

The integration can be performed by the contour integral method, which is essentially similar to that explained in the previous paper (Kato, 1968). The integral paths required in the following calculation are defined in Fig. 2 of that paper. First, the complex function

$$I_m(\pm)=\left(\frac{1}{\beta}\right)^{m-1}\frac{(-z\pm\sqrt{z^2+\beta^2})^m}{\pm\sqrt{z^2+\beta^2}} \times\exp\left[i(\pm\eta_1\sqrt{z^2+\beta^2}-\eta_2 z)\right] \qquad (A3)$$

is introduced. Here, the real part of $\sqrt{z^2+\beta^2}$ is defined as positive for a large positive s^r in the equation $z=s^r+is^i$. The integral sum can be represented as follows:

$$U_m=\int_{L_1+L_2} I_m(+)\mathrm{d}z+\int_{L_3+L_4} I_m(-)\mathrm{d}z\,. \qquad (A4)$$

Under the conditions of $\eta_1\mp\eta_2>0$, since the integrals of $I_m(\pm)$ over the infinite semicircles of $C(\pm)$ are zero, the above sum is reduced to

$$U_m=-\int_{l_1+l_2} I_m(+)\mathrm{d}z-\int_{l_3+l_4} I_m(-)\mathrm{d}z\,. \qquad (A5)$$

Changing the variable z into φ by the relations $z=i\beta\sin\varphi$ on l_1 and l_2 and $z=-i\beta\sin\varphi$ on l_3 and l_4, we have

$$\begin{aligned}U_m&=i\beta\int_0^{2\pi}\exp\left[i\{m\varphi+\beta(\eta_1\cos\varphi+i\eta_2\sin\varphi)\}\right]\mathrm{d}\varphi\\&=i\beta\int_0^{2\pi}\exp\left[i\{m\varphi+\beta\sqrt{\eta_1^2-\eta_2^2}\cos(\varphi+\theta)\}\right]\mathrm{d}\varphi\\&=2\pi i^{m+1}\beta J_m(\beta\sqrt{\eta_1^2-\eta_2^2})e^{-im\theta},\ (\eta_1\pm\eta_2>0)\,. \qquad (A6)\end{aligned}$$

Here, θ is introduced by the relation

$$\eta_1\cos\varphi+i\eta_2\sin\varphi=\sqrt{\eta_1^2-\eta_2^2}\cos(\varphi+\theta)\,. \qquad (A7)$$

The explicit form of $e^{-im\theta}$ will be given later.

In the case of $\eta_1\mp\eta_2<0$, the same procedures can be used for obtaining U_m by integrating $I_m(\pm)$ over the contours $C(\mp)$. Thus, we shall have

$$\begin{aligned}U_m&=-\int_{l_3+l_4} I_m(+)\mathrm{d}z-\int_{l_1+l_2} I_m(-)\mathrm{d}z\\&=\int_{l_3+l_4} I_m(-)\mathrm{d}z+\int_{l_1+l_2} I_m(+)\mathrm{d}z\\&=-2\pi i^{m+1}\beta J_m(\beta\sqrt{\eta_1^2-\eta_2^2})e^{-im\theta},\ (\eta_1\pm\eta_2<0). \qquad (A8)\end{aligned}$$

In other two cases of $\eta_1^2-\eta_2^2<0$, taking either one of the contours $C(+)$ and $C(-)$ for integrating $I_m(+)$ and $I_m(-)$, we obtain

$$U_m=0,\ (\eta_1^2-\eta_2^2<0)\,. \qquad (A9)$$

Now, we shall evaluate the factor $e^{-im\theta}$ in equations ($A6$) and ($A8$). From equation ($A7$) the following relations are obtained

$$\cos\theta=\frac{\eta_1}{\sqrt{\eta_1^2-\eta_2^2}} \qquad (A10a)$$

$$\sin\theta=-i\frac{\eta_2}{\sqrt{\eta_1^2-\eta_2^2}}\,. \qquad (A10b)$$

Consequently, we obtain that

$$e^{-im\theta}=\left(\frac{\eta_1-\eta_2}{\eta_1+\eta_2}\right)^{\frac{m}{2}},\ (\eta_1\pm\eta_2>0) \qquad (A11a)$$

$$e^{-im\theta}=(-1)^m\left(\frac{\eta_1-\eta_2}{\eta_1+\eta_2}\right)^{\frac{m}{2}},\ (\eta_1\pm\eta_2<0)\,. \qquad (A11b)$$

Substituting equations ($A11a$ and b) into equations ($A6$) and ($A8$) respectively, we obtain

$$U_m=2\pi i^{m+1}\beta\left(\frac{\eta_1-\eta_2}{\eta_1+\eta_2}\right)^{\frac{m}{2}}J_m(\beta\sqrt{\eta_1^2-\eta_2^2}),\quad(\eta_1\pm\eta_2>0) \qquad (A12a)$$

$$U_m=2\pi i^{m+1}(-1)^{m+1}\beta\left(\frac{\eta_1-\eta_2}{\eta_1+\eta_2}\right)^{\frac{m}{2}}J_m(\beta\sqrt{\eta_1^2-\eta_2^2}),\quad(\eta_1\pm\eta_2<0)\,. \qquad (A12b)$$

In the case of Type II, the following integrals appear instead of $U_m(\pm)$, calculated above.

$$V_m(\pm)=\left(\frac{1}{\beta}\right)^{m-1}\int_{-\infty}^{+\infty}\frac{(s\pm\sqrt{s^2+\beta^2})^m}{\pm\sqrt{s^2+\beta^2}} \times\exp\left[i(\pm\eta_1\sqrt{s^2+\beta^2}-\eta_2 s)\right]\mathrm{d}s^r. \qquad (A13)$$

They are transformed to $U_m(\pm)$ simply by changing the sign of η_2. Thus, we have

$$V_m=2\pi i^{m+1}\beta\left(\frac{\eta_1+\eta_2}{\eta_1-\eta_2}\right)^{\frac{m}{2}}J_m(\beta\sqrt{\eta_1^2-\eta_2^2}),\quad(\eta_1\pm\eta_2>0) \qquad (A14a)$$

$$V_m=2\pi i^{m+1}(-1)^{m+1}\beta\left(\frac{\eta_1+\eta_2}{\eta_1-\eta_2}\right)^{\frac{m}{2}}J_m(\beta\sqrt{\eta_1^2-\eta_2^2}),\quad(\eta_1\pm\eta_2<0)\,. \qquad (A14b)$$

In the above calculation it is implicitly assumed that the real part of β, β^r, is positive. Even when β^r is negative, however, the procedure is essentially identical. In this case, the integral sums U_m and V_m are again given by equations ($A12$) and ($A14$) respectively.

The spherical-wave solutions in vacuum are expressed by the linear combination of the functions U_m and U_{m+2} for the cases of Type I, and of V_m and V_{m+2} for the cases of Type II provided that the arguments η_1 and η_2 are replaced by ζ_1 and ζ_2.

APPENDIX *B*

The phase terms of the plane-wave solutions†

(*a*) *Type* I

The phase of the wave field, equation (29*a*), is rearranged in the form

$$\bar{\varphi}_r=\{(\mathbf{k}_0-\mathbf{K}_e)\,.\,(\mathbf{r}-\mathbf{r}_e)\}+\{(\mathbf{k}_{0,r}-\mathbf{k}_0)\,.\,(\mathbf{r}-\mathbf{r}_a)\}+(\mathbf{K}_e\,.\,\mathbf{r})\,. \qquad (B1)$$

In this expression, $\mathbf{r}_e$ and $\mathbf{r}_a$ are arbitrary provided that they lie on the entrance and exit surfaces respectively. For this reason, in the following calculation $\mathbf{r}_e$ is fixed at the entrance point E and $\mathbf{r}_a$ is fixed at either $\bar{A}$ or $\bar{A}^*$, defined in Fig. 3(*a*).

By the use of the oblique coordinate axes $\hat{\mathbf{K}}_0$ and $\hat{\mathbf{K}}_g$, one can write the differences of the position vectors,

$$\mathbf{r}-\mathbf{r}_e=l_0\hat{\mathbf{K}}_0+l_g\hat{\mathbf{K}}_g \qquad (B2)$$

$$\mathbf{r}-\mathbf{r}_a=l_0\hat{\mathbf{K}}_0+l_{g,r}\hat{\mathbf{K}}_g \quad (\mathbf{r}_a \text{ fixed at } \bar{A}) \qquad (B3a)$$

$$=l_{0,r}\hat{\mathbf{K}}_0+l_g\hat{\mathbf{K}}_g \quad (\mathbf{r}_a \text{ fixed at } \bar{A}^*) \qquad (B3b)$$

where l_0, l_g, $l_{0,r}$ and $l_{g,r}$ are the oblique coordinates defined in Fig. 3(*a*). From Fig. 2, it is seen that

$$\mathbf{k}_0-\mathbf{K}_e=\overrightarrow{DE}=\overrightarrow{DL}+\overrightarrow{L\bar{L}}+\overrightarrow{\bar{L}E}$$

$$\mathbf{k}_{0,r}-\mathbf{k}_0=\overrightarrow{D_rD}=\overrightarrow{D_rL}-\overrightarrow{DL}$$

where $\overrightarrow{DL}=(\mathbf{k}_0-\bar{\mathbf{k}}_0)$ and $\overrightarrow{D_rL}=(\mathbf{k}_{0,r}-\bar{\mathbf{k}}_0)$ and $\overrightarrow{\bar{L}E}=-\mathbf{K}_x$. Thus, we shall have, by the virtue of the definitions of Resonanzfehler [equations (15 and 22)]

$$\bar{\varphi}_r=\bar{\varphi}+\Delta\eta_g(l_g-l_{g,r})+\Delta\eta_{0,r}l_0+\Delta\eta_{g,r}l_{g,r} \qquad (B4a)$$

$$=\bar{\varphi}+\Delta\eta_0(l_0-l_{0,r})+\Delta\eta_{g,r}l_g+\Delta\eta_{0,r}l_{0,r} \qquad (B4b)$$

where

$$\bar{\varphi}=K_yy+K_zz+\tfrac{1}{2}K\chi_0(l_0+l_g)\,. \qquad (B5)$$

In deriving these we used $(\mathbf{K}_e\,.\,\mathbf{r})=K_xx+K_yy+K_zz$; $K_xx-[\mathbf{K}_x\,.\,(\mathbf{r}-\mathbf{r}_e)]=0$; $(\overrightarrow{L\bar{L}}\,.\,\hat{\mathbf{K}}_0)=(\overrightarrow{L\bar{L}}\,.\,\hat{\mathbf{K}}_g)=\frac{1}{2}K\chi_0$. In equation (*B*5), the term $\frac{1}{2}K\chi_0(l_0+l_g)$ is the phase P defined in equation (14) [see equation (31) of Kato, 1968].

As shown in equation (31*a*), $\bar{\varphi}_r$ is rewritten as

$$\bar{\varphi}_r=\bar{\varphi}\pm\eta_1\sqrt{s^2+\beta^2}-\eta_2 s \qquad (B6)$$

where η_1 and η_2 are the functions of l_0, l_g *etc.* As was seen in Appendix *A*, we need only the expressions for $\eta_1\pm\eta_2$. For this purpose, we notice in equations (*B*4*a* and *b*) that $\Delta\eta_{0,r}$ and $\Delta\eta_{g,r}$ are proportional to $\Delta\eta_g$ and $\Delta\eta_0$ respectively [see equations (27)], and that the terms proportional to $\Delta\eta_0$ and $\Delta\eta_g$ are irrelevant in obtaining $\eta_1+\eta_2$ and $\eta_1-\eta_2$ respectively (see Table 4). We, therefore, see that

$$[\bar{\varphi}_r]_+=\Delta\eta_{0,r}l_{0,r} \qquad (B7a)$$

$$[\bar{\varphi}_r]_-=\Delta\eta_{g,r}l_{g,r} \qquad (B7b)$$

where $[\,]_+$ and $[\,]_-$ are the operators used to select the relevant terms. Thus, finally we obtain

$$\eta_1+\eta_2=-\frac{\gamma_0'}{\gamma_g'}l_{0,r}\sin 2\theta_B=-\frac{\gamma_0'}{\gamma_g'}x_{g,r} \qquad (B8a)$$

$$\eta_1-\eta_2=-\frac{\gamma_0}{\gamma_g}\frac{\gamma_g'}{\gamma_0'}l_{g,r}\sin 2\theta_B=-\frac{\gamma_0}{\gamma_g}\frac{\gamma_g'}{\gamma_0'}x_{0,r} \qquad (B8b)$$

where $x_{0,r}$ and $x_{g,r}$ are the perpendiculars to the lines JJ' and LL' from the observation point P in Fig. 3(*a*). The signs of $x_{0,r}$ and $x_{g,r}$ are determined by those of $l_{g,r}$ and $l_{0,r}$ respectively.

(*b*) *Type* II

The same treatment can be applied to the case of Type II. The results are simply obtained by using the geometrical factors γ_0'' and γ_g'' instead of γ_0' and γ_g' in equations (*B*8*a* and *b*); *i.e.*

$$\eta_1+\eta_2=-\frac{\gamma_0''}{\gamma_g''}x_{g,r} \qquad (B9a)$$

$$\eta_1-\eta_2=-\frac{\gamma_0}{\gamma_g}\frac{\gamma_g''}{\gamma_0''}x_{0,r} \qquad (B9b)$$

where $x_{0,r}$ and $x_{g,r}$ are the perpendiculars to the lines JJ' and LL' from the observation point P in Fig. 3(*b*)

(*c*) *The penetrating wave fields in vacuum*

In Type I, the phase $\bar{\varphi}_{g,t}$ in equation (29*c*) is reduced to the following form by the use of equation (18*c*),

$$\bar{\varphi}_{g,t}=\bar{\varphi}+K\delta_gt_a+\Delta\eta_0l_0+\Delta\eta_gl_g+2\pi(\mathbf{g}\,.\,\mathbf{r}) \qquad (B10)$$

where the form of $K\delta_g$ is given in Table 2. Incidentally, the expression (34) of the constant phase P_g is straightforwardly obtained from equation (*B*10).

Using operators $[\,]_+$ and $[\,]_-$ on $\bar{\varphi}_{g,t}$, we obtain

$$[\bar{\varphi}_{g,t}]_+=\Delta\eta_gl_g+[K\delta_gt_a]_+=\Delta\eta_g(l_g-t_a/\gamma_g') \qquad (B11a)$$

$$[\bar{\varphi}_{g,t}]_-=\Delta\eta_0l_0\,. \qquad (B11b)$$

From these, equations (55) for $\zeta_1\pm\zeta_2$ are obtained.

In Type II, the phase in equation (39*c*) is given by

$$\bar{\varphi}_{0,t}=\bar{\varphi}+K\delta_0t_b+\Delta l_0\eta_0+\Delta\eta_gl_g \qquad (B12)$$

where the relation $\mathbf{K}_{0,t}=\mathbf{k}_0+K\delta_0\mathbf{n}_b$ is used and $K\delta_0$ is given in Table 2. It follows, therefore, that

$$[\bar{\varphi}_{0,t}]_+=\Delta\eta_gl_g \qquad (B13a)$$

$$[\bar{\varphi}_{0,t}]_-=\Delta\eta_0l_0+[K\delta_0t_b]_-=\Delta\eta_0(l_0-t_b/\gamma_0'')\,. \qquad (B13b)$$

From equations (*B*12) and (*B*13*a* and *b*), the expressions (44) and (56*a* and *b*) are obtained for P_0 and $\zeta_1\pm\zeta_2$ respectively.

† This appendix is given to show the method for finding the expressions for the phases in the Laue–Bragg cases. The principle involved is useful in multiple reflexion problems such as in the case of Laue–(Bragg)^m.

References

BORRMANN, G., HILDEBRANDT, G. & WAGNER, H. (1955). *Z. Phys.* **142**, 406.
BORRMANN, G. & LEHMANN, K. (1963). *Crystallography and Crystal Perfection.* p. 101. London: Academic Press.
EWALD, P. P. (1916). *Ann. Physik*, **49**, 117.
KATO, N. (1961*a*). *Acta Cryst.* **14**, 526.
KATO, N. (1961*b*). *Acta Cryst.* **14**, 627.
KATO, N. (1968). *J. Appl. Phys.* **39**, 2225.
KATO, N. & LANG, A. R. (1959). *Acta Cryst.* **12**, 787.
KATO, N., USAMI, K. & KATAGAWA, T. (1967). *Advanc. X-ray Analysis*, **10**, 46.
LAUE, M. VON (1960). *Röntgenstrahlinterferenzen.* Frankfurt: Akademische Verlagsgesellschaft.
LEHMANN, K. & BORRMANN, G. (1967). *Z. Kristallogr.* **125**, 234.
TAKAGI, S. (1969). *J. Phys. Soc. Japan*, **26**, 1239.
URAGAMI, T. (1969). *J. Phys. Soc. Japan*, **27**, 147.
URAGAMI, T. (1970). *J. Phys. Soc. Japan*, **28**, 1508.
URAGAMI, T. (1971). *J. Phys. Soc. Japan*, **31**, 1141.
ZACHARIASEN, W. H. (1945). *Theory of X-ray Diffraction in Crystals.* New York: John Wiley.

Acta Cryst. (1972). A**28**, 113

The Theory of X-ray Crystal Diffraction for Finite Polyhedral Crystals. II. The Laue–(Bragg)^m Cases

BY T. SAKA, T. KATAGAWA AND N. KATO

Department of Applied Physics, Faculty of Engineering, Nagoya University, Nagoya, Japan

(*Received* 18 *January* 1971 *and in revised form* 7 *July* 1971)

The wave fields specified by the Laue–(Bragg)^m cases are treated from the view points of the plane-wave and spherical-wave theory. The results are very similar to those in the Laue–Bragg case in Part I (*Acta Cryst.* (1972). A**28**, 102.). The diffraction phenomena for a finite polyhedral crystal and the experiment of Lehmann & Borrmann (*Z. Kristallogr.* (1967). **125**, 234) are discussed from the view point of the spherical-wave theory.

Introduction

When the exit surfaces, S_a and S_b, are close to each other the Laue–Bragg waves obtained previously may be reflected many times at them before leaving through any one of the exit surfaces. In this Part, this topic is treated from the stand points of both the plane-wave and spherical-wave theories. According to the terminology defined in Part I (Saka, Katagawa & Kato, 1972), this case is specified as the Laue–(Bragg)^m case. The same notations as in Part I are used in this Part, unless otherwise specified. The equations of Part I are cited by adding I to the equation number.

Here, again, two cases of Type I and II must be distinguished. In the former case, the crystal waves hit the exit surfaces in the sequence, S_a, S_b, S_a, ..., whereas the sequence starts from S_b in the latter case (see Fig. 1). In order to specify the quantities pertinent to the wave fields reflected m times, the suffix m is added to them, *e.g.* the wave vector $\mathbf{k}_{0,m}$ and Anpassung δ_m. Obviously, $\mathbf{k}_{0,0}$, $\mathbf{k}_{0,1}$ and δ_1 are $\mathbf{k}_0$, $\mathbf{k}_{0,r}$ and δ_r in Part I.

The wave fields of Type I

As shown in Fig. 1(*a*), the waves reflected $2n$ and $2n+1$ times fall on the exit surfaces S_a and S_b respectively. The boundary conditions for the totally reflected waves are read as,

$$0=d_{0,2n}\exp[i(\mathbf{k}_{0,2n}\cdot\mathbf{r}_{a,2n+1})]+d_{0,2n+1}\exp[i(\mathbf{k}_{0,2n+1}\cdot\mathbf{r}_{a,2n+1})] \quad (1a)$$

$$0=d_{g,2n+1}\exp[i(\mathbf{k}_{g,2n+1}\cdot\mathbf{r}_{b,2n+2})]+d_{g,2n+2}\exp[i(\mathbf{k}_{g,2n+2}\cdot\mathbf{r}_{b,2n+2})] \quad (1b)$$

where $\mathbf{r}_{a,2n+1}$ and $\mathbf{r}_{b,2n+2}$ denote position vectors on the surfaces S_a and S_b.

From these equations, one can obtain the recurrence formulae

$$d_{0,2n+1}=-d_{0,2n}\exp[i\{(\mathbf{k}_{0,2n}-\mathbf{k}_{0,2n+1})\cdot\mathbf{r}_{a,2n+1}\}] \quad (2a)$$

$$d_{0,2n+2}=-\frac{\Delta\eta_{0,2n+1}}{\Delta\eta_{0,2n+2}}d_{0,2n+1}\times\exp[i\{(\mathbf{k}_{0,2n+1}-\mathbf{k}_{0,2n+2})\cdot\mathbf{r}_{b,2n+2}\}]. \quad (2b)$$

In the last equation, the relations $\mathbf{k}_{g,m}=\mathbf{k}_{0,m}+2\pi\mathbf{g}$ and $d_{g,m}/d_{0,m}=2\Delta\eta_{0,m}/KC\chi_{-g}$ are used, where $\Delta\eta_{0,m}$ is the Resonanzfehler of the wave reflected m times. By combining these, it is easy to see that